Research Square

Preprints are preliminary reports that have not undergone peer review.
They should not be considered conclusive, used to inform clinical practice,
or referenced by the media as validated information.

Molecular and evolutionary characterization of feline panleukopenia virus using bioinformatics tools

Luiza dos Santos Miranda
Universidade de Caxias do Sul (UCS), Caxias do Sul
Rafael Sartori Flores
Universidade de Caxias do Sul (UCS), Caxias do Sul
Júlia da Silva Ramos
Universidade de Caxias do Sul (UCS), Caxias do Sul
Nicole Amoêdo Luvison
Universidade de Caxias do Sul (UCS), Caxias do Sul
Ketlin Milena Zardin
Universidade de Caxias do Sul (UCS), Caxias do Sul
Pedro Augusto Freire de Sá Pontes
Universidade de Caxias do Sul (UCS), Caxias do Sul
João Pedro Lunardi Bedin
Universidade de Caxias do Sul (UCS), Caxias do Sul
Tamiris Silva Lopes
Universidade de Caxias do Sul (UCS), Caxias do Sul
Vagner Ricardo Lunge
Universidade de Caxias do Sul (UCS), Caxias do Sul
André Felipe Streck
afstreck@ucs.br

Universidade de Caxias do Sul (UCS), Caxias do Sul

Research Article

Keywords: FPV, molecular evolution, phylogeny, selective pressure, vaccines

Posted Date: April 7th, 2026

DOI: https://doi.org/10.21203/rs.3.rs-8767944/v1

License: This work is licensed under a Creative Commons Attribution 4.0 International License.
Read Full License

Additional Declarations: No competing interests reported.

Abstract

Feline panleukopenia virus (FPV) is a highly contagious parvovirus that continues to cause significant disease in domestic and wild felids worldwide. Although historically considered genetically stable and effectively controlled by vaccination, recent molecular studies have expanded the available genomic data, prompting renewed interest in its evolutionary dynamics. Here, we conducted a global bioinformatic analysis of FPV genetic diversity, evolution and antigenic constraints using 446 complete VP2 sequences collected between 1967 and 2023. Phylogenetic analysis identified nine major clades (A–I) with distinct geographic and temporal patterns, while vaccine strains consistently clustered within a single clade. Overall VP2 variability was low, with most amino acid substitutions occurring sporadically and only two sites exceeding 5% frequency. Selective pressure analysis detected a single codon under weak positive selection, consistent with strong purifying selection acting on the capsid. Molecular clock and Bayesian skyline analyses indicated a slow evolutionary rate and a relatively stable effective population size over time. Structural and epitope analyses showed that residues with higher predicted antigenicity were significantly more conserved, and all predicted high-affinity cytotoxic T-lymphocyte epitopes remained unchanged across sequences. These results indicate that FPV evolution is highly constrained and that no evidence of emerging antigenic variants of concern is currently detectable, supporting the continued effectiveness of existing vaccines and the importance of ongoing molecular surveillance.

Introduction

Feline panleukopenia virus (FPV), a member of the *Parvoviridae* family, is the causative agent of a highly contagious and often fatal disease in cats, particularly affecting kittens (Parrish 1999, Ikeda et al. 2000). Despite the availability of effective attenuated and inactivated vaccines, outbreaks continue to occur in domestic and shelter populations worldwide (Rehme et al. 2022). This persistent circulation is partly attributed to incomplete vaccination coverage, but also to the existence of naturally occurring viral variants whose epidemiological relevance is still not fully understood.

The major capsid protein VP2 is responsible for receptor binding, host range, and antigenicity, and remains the primary target of neutralizing antibodies (Parker and Parrish 1997). Historically, FPV has been described as a genetically stable virus, with a mutation rate considerably lower than that of its derivative, canine parvovirus type 2 (CPV-2) (Truyen and Parrish 2013). This genomic stability is one of the reasons why FPV vaccines have remained effective for decades and why major antigenic shifts have not been documented in vaccine strains.

However, molecular analyses conducted over the past decades consistently demonstrate that feline panleukopenia virus (FPV) exhibits a highly conserved genetic structure, particularly within the VP2 capsid protein (Decaro 2008). Although sporadic amino acid substitutions have been described in individual field strains, these changes are typically rare, non-fixed, and lack evidence of antigenic or

functional consequences. To date, there is no indication that such substitutions reflect ongoing antigenic drift, host adaptation, or compromised vaccine efficacy (Pan et al. 2023).

Advances in bioinformatics have made it possible to evaluate viral evolution with high resolution. Nevertheless, comprehensive global analyses of FPV remain limited, and several geographic regions are still underrepresented in genomic databases, hindering robust assessments of viral diversity and evolutionary trends.

This study aims to investigate the genetic diversity, evolutionary patterns, and population dynamics of FPV using an extensive dataset and multiple bioinformatics approaches, providing updated insights relevant to molecular surveillance and immunoprophylaxis.

Materials and Methods

Collection of Viral Sequences

All complete feline panleukopenia virus (FPV) sequences available from 1967 to 2023 were retrieved from the GenBank database between May and July 2024, (n = 446); repeated and incomplete sequences were excluded. The ancestral strain was considered as the reference sequence (EU659111.1: USA Cat – 1967), and the vaccine strains EU498680.1 (Purevax – 2008), EU498681.1 (Felocell – 2008), and OQ615264.1 (Nobivac – 2023) were also included. The VP2 region of each sequence was extracted and are presented in Appendix A.

Alignment and Substitution Analysis

The FASTA file was aligned in MEGA11 (Kumar et al., 2021) and the sequences were renamed according to country of origin and collection year. The aligned file was saved in ".meg" format and subsequently opened in Geneious for amino acid substitution analysis. The ancestral strain (EU659111.1, 1967) was used as the reference for comparison with all other collected sequences. Based on these analyses, a substitution table was generated in Excel relative to the ancestral sequence.

Phylogenetic Tree Construction

To investigate the temporal and geographical distribution of FPV strains, a phylogenetic tree was constructed in MEGA11. The tree was generated with all collected sequences using the Maximum Likelihood method under the Hasegawa-Kishino-Yano model, with 1000 bootstrap replications. The model was selected by the software as the best fit. Sequences from each clade of the phylogenetic tree were extracted into separate Notepad files, labeled with year and country of origin. Arithmetic means of the collection years, standard deviations, and the percentage of sequences per continent were calculated, resulting in a comparative table. The Notepad files were saved in FASTA format and organized into respective folders in Geneious. Each group of sequences was edited in nucleotide view, generating a consensus sequence for each clade. Subsequently, a new folder was created in Geneious containing all consensus sequences, along with the ancestral and vaccine strains, for comparative

purposes. A table was produced showing substitutions relative to the ancestral and vaccine strains, and graphs were generated to aid visualization.

Selection Pressure Analysis

Selection pressure analysis was performed using Datamonkey (http://www.datamonkey.org), applying the Single-Likelihood Ancestor Counting (SLAC), Fast Unconstrained Bayesian Approximation (FUBAR), and Mixed Effects Model of Evolution (MEME) methods. A site was considered under positive selection only when identified by at least two of the three algorithms, and deemed significant when meeting the following thresholds: $p < 0.1$ in SLAC, $p < 0.05$ in MEME, and posterior probability > 0.9 in FUBAR.

Removal of Duplicate and Recombinant Sequences

All sequences were analyzed in TempEst to identify and exclude problematic, erroneous, or recombinant sequences. The filtered sequences were realigned in MEGA11 and saved in FASTA format for molecular clock and population dynamics analyses. A detailed table of these sequences, including accession number, country of origin, host, and collection year, is provided in Appendix B.

Molecular Clock Analysis

To infer divergence times and substitution rates of the 268 selected FPV sequences, BEAST2 v1.10.4 was employed, implementing Bayesian inference via Markov Chain Monte Carlo (MCMC) (Suchard et al. 2018). A relaxed molecular clock with lognormal distribution and the HKY+G substitution model were used, based on prior model selection. Phylogenetic reconstruction was based on a coalescent constant population model. MCMC chains were run for 50,000,000 generations, sampling every 1,000 generations, with the first 10% discarded as burn-in. Output files were analyzed in Tracer v1.7.1 to assess chain convergence and estimate mean values and 95% highest posterior density (HPD) intervals for parameters of interest, particularly tree height (tree.height) and mean substitution rate (rate.mean).

Population Dynamics

Population dynamics analysis of FPV was performed in BEAST2 using the Coalescent Bayesian Skyline (CBS) model. The best-fit nucleotide substitution model (TPM3u+F+I+R2) and the molecular clock model were employed. MCMC chains were run for 100,000,000 iterations, with sampling every 10,000 steps. The resulting log files were examined in Tracer v1.7 to confirm adequate convergence, verifying that the effective sample size (ESS) exceeded 250 for all estimated parameters after a 10% burn-in.

Epitope prediction

Linear B-cell epitope scores were generated using BepiPred-3.0 (DTU HealthTech). The VP2 reference sequence was submitted to the online predictor (https://services.healthtech.dtu.dk). Scores were integrated into a position-by-position dataset and matched with mutation frequencies.

Cytotoxic T-lymphocyte (CTL) epitope prediction was performed using NetMHC 4.0 (DTU HealthTech) under the HLA-A0201 allele. Although FPV infects felids, HLA-A0201 was selected as a representative model to explore the general relationship between predicted class I–restricted epitopes and observed evolutionary variation. NetMHC was configured to analyze all overlapping 9-mer peptides in VP2, and peptides with a %Rank ≤ 0.5 were classified as strong binders, whereas those with %Rank ≤ 2.0 were considered weak binders. Each predicted epitope was mapped to its corresponding coordinate interval along VP2, and residues falling within any predicted 9-mer were labeled as “epitope positions.” All remaining residues were categorized as “non-epitope positions.”

Statistical analyses

Statistical analyses were conducted to determine whether antigenicity and epitope location were associated with natural viral variability. All analyses were performed in R 4.4.1. BepiPred-3.0 conformational and linear epitope scores (0–1) were compared between residues with and without amino-acid substitutions. Because score distributions were non-normal (Shapiro–Wilk test), group differences were assessed using Mann–Whitney U tests. Median values and sample sizes were reported for each comparison. Data were visualized as boxplots with overlaid jittered dots, and p-values were annotated on the plots.

Additionally, a logistic regression model was constructed to evaluate whether antigenicity predicted the likelihood that a residue exhibited at least one mutation across all GenBank sequences. For this model, the binary response variable indicated whether a position was mutated (1) or conserved (0), and the predictor variable was the continuous BepiPred-3.0 score.

Results

Amino acid substitutions observed in VP2

Analysis of the 446 FPV VP2 sequences revealed 149 positions containing at least one amino acid substitution relative to the ancestral 1967 strain. Overall variability was low: 132 sites showed mutations in only one to five sequences, indicating sporadic, non-fixed events. Only two positions exhibited higher frequencies: A91S, detected in 24.9% of the sequences, and V232I, present in 9.2%. These findings confirm the high genetic and structural stability of VP2, a hallmark of FPV evolution. The distribution of substitutions across the VP2 protein is shown in Figure 1. Most mutations occurred in a scattered pattern, with no clear clustering in specific structural or antigenic regions.

Comparing the consensus sequences of the nine phylogenetic clades with the ancestral strain, only one recurrent clade-specific mutation was detected: A91S, exclusive to clade D. In contrast, the three commercial vaccine strains shared a distinct mutational profile, harboring T101I, V232I, and V562L, all absent from the field clades. These substitutions likely reflect adaptations associated with the attenuation process. A detailed comparison is provided in Table 1.

Table 1 – Comparison between ancestral, vaccine, and clade consensus sequences

Vaccine strains and clades	91	101	232	562
Ancestral (EU659111.1 - Clade I)	A	T	V	V
Felocell (EU498681.1 - Clade B)	.	.	I	L
Nobivac (OQ615264.1 - Clade B)	.	.	I	L
Purevax (EU498680.1 – Clade B)	.	I	I	L
Clade A	.	.	.	.
Clade B	.	.	.	.
Clade C	.	.	.	.
Clade D	S	.	.	.
Clade E	.	.	.	.
Clade F	.	.	.	.
Clade G	.	.	.	.
Clade H	.	.	.	.
Clade I	.	.	.	.

Phylogenetic structure and clade distribution

Maximum-likelihood phylogenetic analysis grouped the 446 sequences into nine major clades (A–I) (Figure 2), each displaying distinct geographic and temporal characteristics. Clades A and B consisted predominantly of European strains, with mean sampling years of 2011 and 2014, respectively, suggesting the persistence of older, established lineages in this region. In contrast, clades C through H were composed almost exclusively of Asian sequences, collected primarily between 2015 and 2019, reflecting recent diversification likely associated with intensified molecular surveillance in Asia. Clade I exhibited the greatest geographic heterogeneity, comprising sequences from South America, Africa, Europe, and Asia, indicating broader global circulation. The three commercial vaccine strains—Purevax, Felocell, and Nobivac—clustered consistently within clade B, whereas the ancestral 1967 strain grouped within clade I, emphasizing the long-term evolutionary divergence between vaccine lineages and contemporary field variants. A detailed overview of geographic distribution and mean sampling years for each clade is provided in Figures 3.

Evidence of positive selection

Selective pressure analysis identified a single codon—position 300—under positive selection according to two methods: FUBAR (posterior probability = 0.938) and SLAC (p = 0.0887). No additional positively selected sites were detected by SLAC, FUBAR, or MEME. Mutation frequency at position 300 was 2.47%

among the analyzed sequences. The complete results of the selection analysis are summarized in Table 2.

Table 2 – Results of FPV selective pressure analysis. Only site 300 was identified as being under positive selection by more than one method (SLAC and FUBAR).

Site	Selection	Method	Prob [α < β]	Method	*p*-value
300	Positive	FUBAR*	0.938	SLAC**	0.0887

* Posterior probability > 0.9

** $p < 0.1$

Molecular clock and population dynamics

The molecular clock analysis generated a time-scaled phylogeny in which the sequence groupings were consistent with the clades recovered in the maximum-likelihood tree. The estimated tree height was 61.25, with a 95% Highest Posterior Density (HPD) interval of 59.00–66.38, and the Effective Sample Size (ESS) for this parameter was 681.4. The mean substitution rate was estimated at 4.22×10^{-4} substitutions/site/unit time, with a 95% HPD interval of 2.61×10^{-4} to 5.91×10^{-4}.

Analysis of FPV population dynamics using a Bayesian Skyline Plot indicated changes in effective population size over the sampled period (Figure 4). The curve shows a gradual increase until the mid-2010s, followed by a stabilization pattern. The Bayesian Skyline reconstruction reflects the temporal distribution of the sequences included in the dataset.

Structural Mapping, and Epitope Scores

NETMHC analysis identified a set of predicted HLA-A0201–restricted epitopes across the VP2 protein (Supplementary material). Three peptides were classified as strong binders (SB) based on predicted affinity thresholds: FLENGWVEI (positions 51–59), YTIENSVPV (positions 242–250) and GLPPFLNSL (positions 284–292). The remaining predicted epitopes were classified as weak binders (WB) and included peptides located at positions 63–71, 101–109, 107–115, 129–137, 135–143, 179–187, 315–323, 412–420, 453–461, and 479–487. All predicted epitopes retained their consensus amino acid sequences, and no substitutions were detected within any of the predicted binder cores.

Structural mapping of VP2 highlighted the spatial distribution of amino acid substitutions and the regions associated with higher BepiPred-3.0 epitope scores. In the three-dimensional models, substituted residues appear in red, whereas all remaining residues are shown in grey (Figures 5 A–C). Substitutions were dispersed across multiple structural elements, including β-strands, coils, and loop regions, without forming clusters in specific domains. Independent projections of conformational and linear BepiPred-3.0 scores are also shown in the structural figures, illustrating the locations of residues with higher predicted epitope probabilities along the VP2 surface.

BepiPred-3.0 score distributions for residues with and without substitutions are summarized in Figures 6 A–B. For conformational epitope predictions, residues without substitutions had a median score of 0.224 (n = 435), compared with 0.206 for residues with substitutions (n = 149), with a significant difference between groups (p = 0.013*). For linear epitope predictions, the median scores were 0.236 for residues without substitutions and 0.202 for those with substitutions, also yielding a highly significant difference (p = 0.005*). Each dot in the boxplots represents an individual amino acid position.

Discussion

The global analysis of 446 VP2 sequences confirms that FPV maintains a highly conserved genetic structure, consistent with its long-recognized evolutionary stability. In this dataset, 88% of amino acid substitutions occurred in only one to five sequences, indicating sporadic and non-fixed variation. This pattern is consistent with earlier observations showing that FPV evolves slowly and undergoes minimal antigenic or structural diversification over time (Parrish 1999, Truyen and Parrish 2013, Parrish 1988). In contrast, canine parvovirus type 2 (CPV-2), despite its close genetic relationship with FPV, exhibits a more dynamic evolutionary trajectory, characterized by higher substitution rates and multiple antigenic shifts (2a/2b/2c) (Truyen and Parrish 2013). The marked stability observed in FPV suggests that this virus occupies a long-established and evolutionarily constrained state in domestic and free-roaming cat populations, with limited selective pressure favoring diversification.

Among all detected substitutions, only A91S and V232I exceeded a frequency of 5%. The A91S substitution was restricted to a single phylogenetic clade, suggesting a geographically or temporally localized event. In contrast, V232I was detected exclusively in vaccine-derived strains in the present dataset. Such substitutions in the VP2 capsid protein can arise during virus attenuation and adaptation to cell culture conditions, reflecting selective pressures distinct from those acting on field strains. Neither substitution was observed in contemporary field strains, indicating that these changes do not represent emerging antigenic variants.

Phylogenetic reconstruction identified nine well-supported clades (A–I) with clear geographic and temporal structure. Clades A and B consisted predominantly of European sequences with earlier mean sampling years, consistent with the persistence of older FPV lineages in European cat populations. In contrast, clades C to H were composed almost exclusively of Asian sequences sampled mainly between 2015 and 2020, reflecting increased sequence deposition and regional diversification reported in recent studies (Pan et al. 2023). Clade I was the most heterogeneous, comprising sequences from South America, Africa, Europe and Asia. The coexistence of geographically restricted clades and a globally mixed clade suggests both regional lineage maintenance and ongoing intercontinental movement of FPV, likely facilitated by animal trade, pet movement and shelter-associated transmission. Selective-pressure analyses identified only a single codon (position 300) under weak positive selection. These findings support the view that VP2 is subject to strong functional and structural constraints, limiting adaptive diversification relative to the more plastic evolutionary patterns observed in CPV-2.[7]

Molecular clock analysis estimated an evolutionary rate of 4.22×10^{-4} substitutions/site/year for FPV VP2, with a narrow 95% HPD interval. This estimate is consistent with previously reported rates for FPV and other single-stranded DNA parvoviruses (Shackelton et al. 2005, Streck et al. 2013). The time-scaled phylogeny reproduced the same clade structure observed in the maximum-likelihood analysis, supporting the internal consistency of the phylogenetic and temporal inferences. The estimated tree height, spanning approximately six decades, reinforcing the characterization of FPV as a slowly diverging viral lineage.

Bayesian Skyline analysis revealed a gradual increase in effective population size until approximately 2015, followed by a stabilization phase. This pattern likely reflects both increased FPV circulation associated with growing cat populations and shelter outbreaks, as well as a marked rise in sequence availability driven by advances in sequencing technologies during the same period. However, temporal clustering of GenBank submissions likely contributes to fluctuations in skyline estimates, underscoring the importance of interpreting population-dynamic reconstructions in light of sampling bias.

Epitope prediction analyses showed that residues with higher predicted linear and conformational B-cell epitope scores were significantly more conserved than non-epitope regions. This pattern suggests that evolutionary constraints are strongest within structurally and immunologically relevant regions of VP2, reflecting the need to preserve neutralizing epitopes involved in host interaction and immune recognition (Parker and Parrish 1997). These findings support the sustained efficacy of long-standing FPV vaccines.

All three predicted high-affinity CTL epitopes (positions 51–59, 242–250 and 284–292) were fully conserved across all analyzed sequences. This absence of variability suggests strong functional constraints and provides no evidence for immune-driven escape at these sites. Similar patterns have been reported for FPV and related protoparvoviruses, which exhibit highly constrained evolution and limited evidence of immune-driven diversifying selection, including at putative T-cell epitope regions (Parker and Parrish 1997, Streck et al. 2022). Although CTL predictions were based on the human HLA-A0201 allele rather than feline MHC molecules, the observed conservation remains biologically informative at a comparative and exploratory level, indicating a lack of targeted diversification in putative antigenic regions.

Structural mapping of substitutions onto the VP2 three-dimensional model showed that amino acid changes were dispersed across the capsid surface and did not form clusters or hotspots. Most substitutions occurred outside the major antigenic loops that constitute the principal neutralizing epitopes of parvoviruses (Parker and Parrish 1997). This spatial distribution suggests that the detected mutations are unlikely to affect capsid conformation, receptor binding or antigenicity.

Overall, the clade structure and mutation patterns observed here closely mirror findings from recent large-scale FPV studies. While increased sequence deposition in Asia since 2015 has revealed localized variants, there is no evidence for globally expanding antigenic lineages (Decaro et al. 2008, Pan et al. 2023, Yu et al. 2024, Domingues et al. 2024). Across all available datasets, including the present analysis, mutations with epidemiological relevance remain rare, transient and geographically restricted.

Together, the phylogenetic, structural and epitope-based analyses indicate that FPV continues to circulate as a highly stable virus under strong purifying selection, with no evidence of emerging antigenic variants of concern.

This study is subject to limitations inherent to analyses based on publicly available sequences, including geographic and temporal sampling bias and underrepresentation of certain regions, particularly Africa and parts of South America. In addition, CTL epitope predictions relied on a human MHC model due to the lack of validated feline class I prediction tools and should therefore be interpreted cautiously. Despite these constraints, the dataset represents the most comprehensive global collection currently available and provides robust insights into FPV evolutionary dynamics.

In conclusion, FPV remains a slowly evolving virus characterized by strong purifying selection, minimal nonsynonymous diversification and sustained conservation of key neutralizing and predicted T-cell epitopes. The nine identified clades primarily reflect geographic structure rather than antigenic divergence, and no evidence of immune escape or vaccine mismatch was detected. These findings support the continued effectiveness of current FPV vaccines and highlight the importance of ongoing molecular surveillance to detect rare evolutionary events at an early stage.

Declarations

Author Contribution

L.S.M., R.S.F., J.S.R., N.A.L., K.M.Z., P.A.F.S.P., J.P.L.B. and T.S.L. performed data collection, sequence curation, bioinformatic analyses, and contributed to data interpretation.L.S.M. and R.S.F. drafted the initial version of the manuscript.N.A.L., K.M.Z. and J.S.R. contributed to phylogenetic, molecular clock, and population dynamics analyses.P.A.F.S.P. and J.P.L.B. conducted epitope prediction and structural mapping analyses.V.R.L. contributed to study design, data interpretation, and critical revision of the manuscript.A.F.S. conceived and supervised the study, coordinated the research activities, and critically revised the manuscript for intellectual content.All authors reviewed and approved the final version of the manuscript.

Declarations of interest

The authors declare no conflict of interest.

Funding Declaration

The authors would like to thank the Coordenação de Aperfeiçoamento de Pessoal de Ensino Superior (CAPES), Conselho Nacional de Desenvolvimento Científico e Tecnológico – CNPq (finance Code 001) and Universidade de Caxias do Sul (UCS) for their financial support.

References

1. Decaro N, Desario C, Elia G, Campolo M, Lorusso E, Mari V, et al (2008) Genetic analysis of feline panleukopenia viruses from cats with gastroenteritis. J Gen Virol 91(9):2301–2309.
2. Domingues CF, de Castro TX, do Lago BV, Garcia RCNC (2024) Genetic characterization of the parvovirus full-length VP2 gene in domestic cats in Brazil. Res Vet Sci 170:105186.
3. Hoelzer K, Parrish CR (2010) The emergence of parvoviruses of carnivores. Vet Res 41(6):39.
4. Ikeda Y, Mochizuki M, Naito R, Nakamura K, Miyazawa T, Mikami T, et al (2000) Predominance of canine parvovirus in unvaccinated cat populations and emergence of new antigenic types of CPVs in cats. Virology 278(1):13–19.
5. Pan S, Jiao R, Xu X, et al (2023) Molecular characterization and genetic diversity of parvoviruses prevalent in cats in Central and Eastern China from 2018 to 2022. Front Vet Sci. 2023;10:1218810.
6. Parker JS, Parrish CR (1997) Canine parvovirus host range is determined by the specific conformation of an additional region of the capsid. J Virol 71(12):9214–9222.
7. Parrish CR (1999) Host range relationships and the evolution of canine parvovirus Vet Microbiol 69(1–2):29–40.
8. Parrish CR, Aquadro CF, Strassheim ML, Evermann JF, Sgro JY, Mohammed HO (1988) Rapid antigenic-type replacement and DNA sequence evolution of canine parvovirus. J Virol 62(3):654–660.
9. Rehme T, Krüger M, Truyen U, Hartmann K, Bergmann M, Reese S, et al (2022) Feline panleukopenia outbreaks and risk factors in cats in animal shelters. Viruses 14(6):1248.
10. Shackelton LA, Parrish CR, Truyen U, Holmes EC (2005) The evolution of canine parvovirus: evidence for viral host switching and its implications for viral pathogenesis. J Virol 79(5):2479–2490.
11. Streck AF, Bonatto SL, Homeier T, et al (2013) Evolutionary analysis of porcine parvovirus supports a decrease in viral genetic diversity due to vaccination. J Gen Virol 94(Pt 6):1368–1378.
12. Streck AF, Canal CW, Truyen U (2002) Viral Fitness and Antigenic Determinants of Porcine Parvovirus at the Amino Acid Level of the Capsid Protein J Virol.96(2):e0119821.
13. Suchard MA, Lemey P, Baele G, Ayres DL, Drummond AJ, Rambaut A (2018) Bayesian phylogenetic and phylodynamic data analysis using BEAST 1.10. Virus Evol 4(1):vey016.
14. Truyen U, Parrish CR (2013) Feline panleukopenia virus: its interesting evolution and current problems in immunoprophylaxis against a serious pathogen. Vet Microbiol 165(1–2):29–32.
15. Yu Z, Wang W, Yu C, He L, Ding K, Shang K, Chen S (2024) Molecular Characterization of Feline Parvovirus from Domestic Cats in Henan Province, China from 2020 to 2022. Vet Sci 11(7):292.

Figures

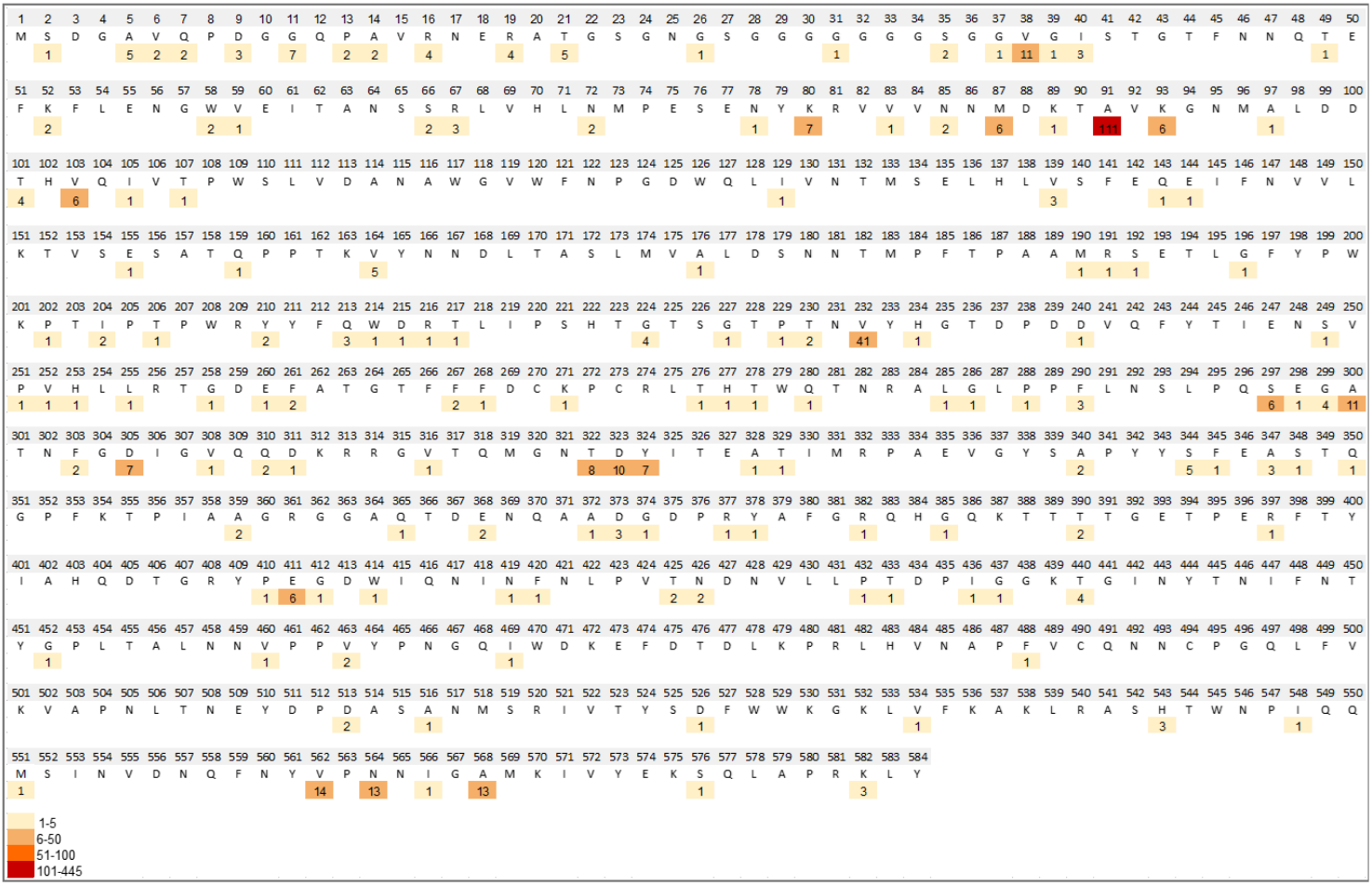


Figure 1

Frequency of amino acid substitutions in the VP2 protein sites of FPV compared to the ancestral strain. The first line shows the amino acid positions, and the second shows the corresponding residues of the reference sequence (ancestral strain). The substitutions identified at each site were represented by a color gradient, categorized according to the observed frequency: 1–5, 6–50, 51–100, and 101–445 sequences containing the same substitution.

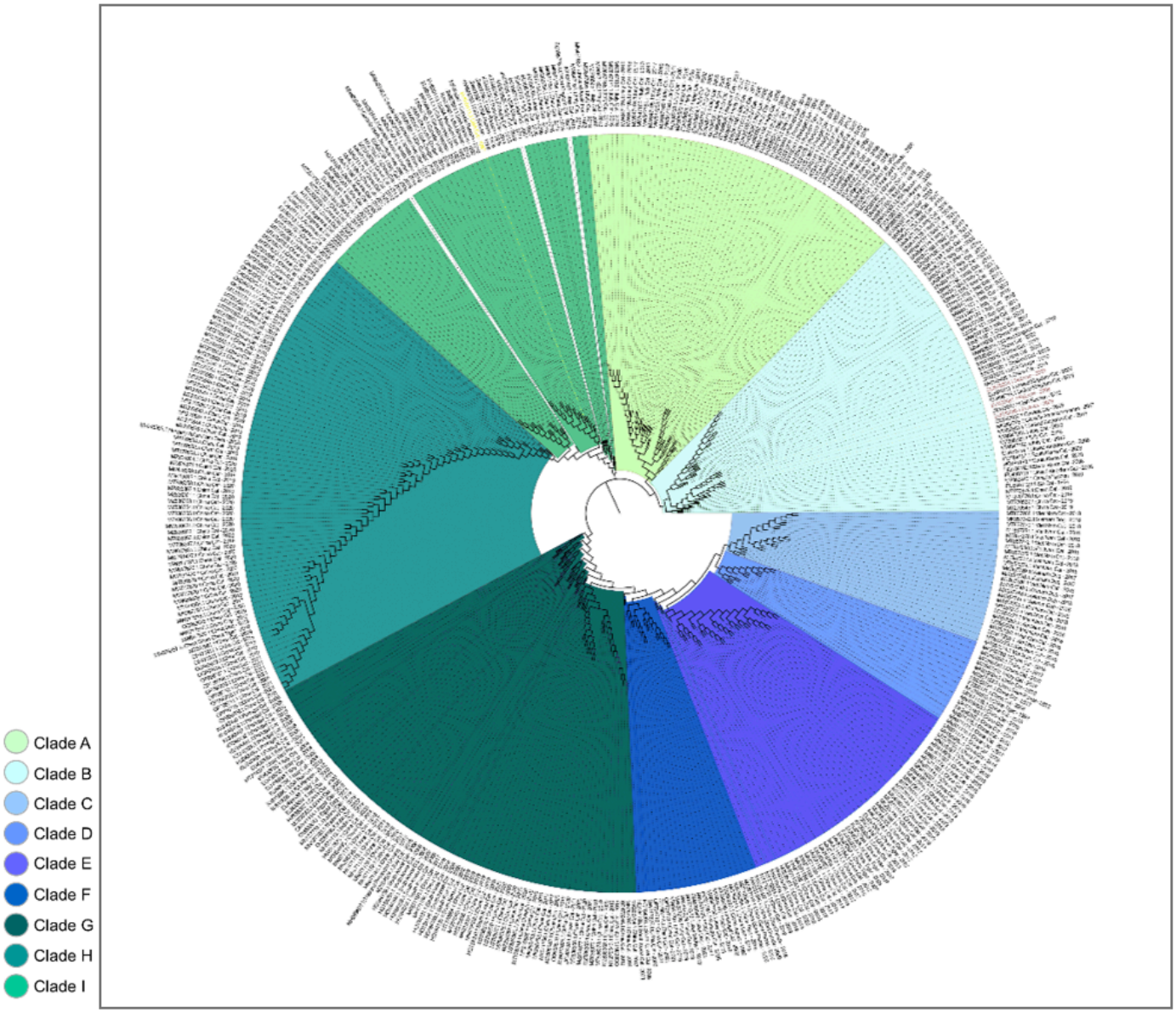


Figure 2

Phylogenetic tree generated using MEGA11 software, including 446 FPV sequences retrieved from the GenBank database, dated between 1967 and 2023. The nine clades of the tree (A–I) are indicated by distinct colors and reflect groupings based on the geographic and temporal distribution of the samples. The three included vaccine strains (Purevax, Felocell, Nobivac) are located in clade B and highlighted in red, while the ancestral strain (USA Cat – 1967) is placed in clade I and highlighted in blue.

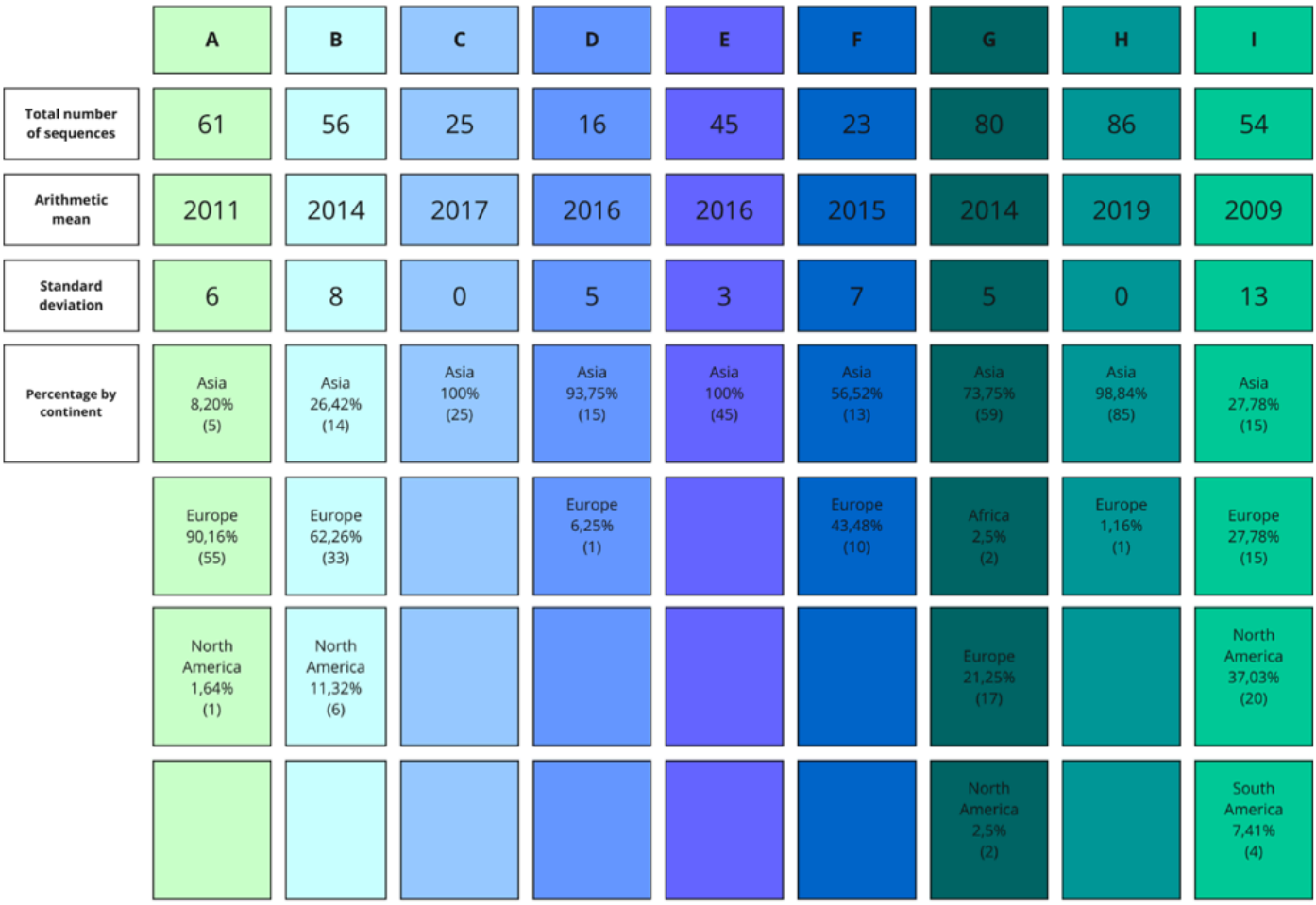


Figure 3

Average year of collection and origin of sequences for each clade.

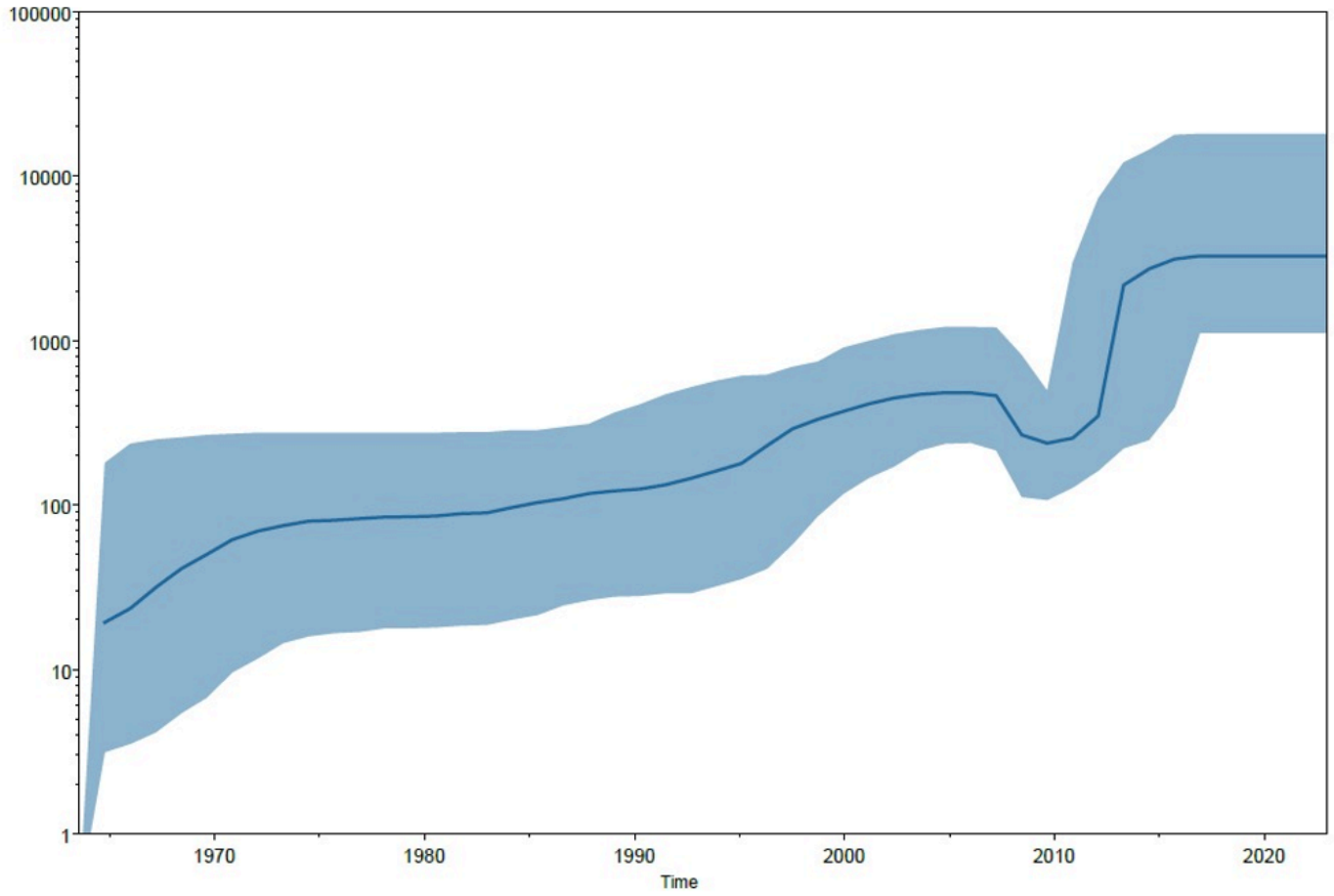


Figure 4

Population dynamics of FPV represented by a Bayesian Skyline Plot generated by BEAST2 software. A relatively steady increase in the viral diversity is observed over the years.

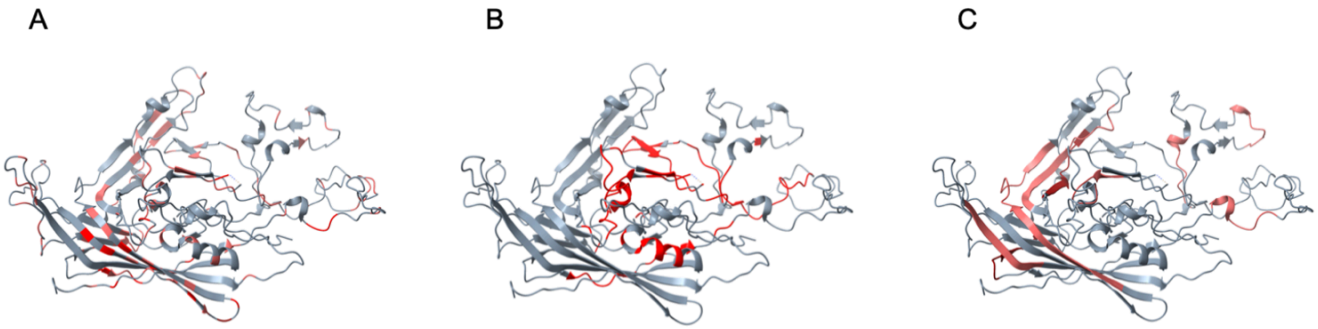


Figure 5

Three-dimensional structural mapping of sequence variation and predicted antigenicity in VP2 protein. (A) Substitution density across the VP2 structure (grey: no substitutions; bright red: 1–5; red: 6–50; dark red: >50). (B) B-cell epitope predictions from BepiPred-3.0, showing non-epitopes in grey and predicted

epitopes in red. (C) NetMHCpan T-cell binding classification (grey: non-binders; bright red: weak binders; dark red: strong binders).

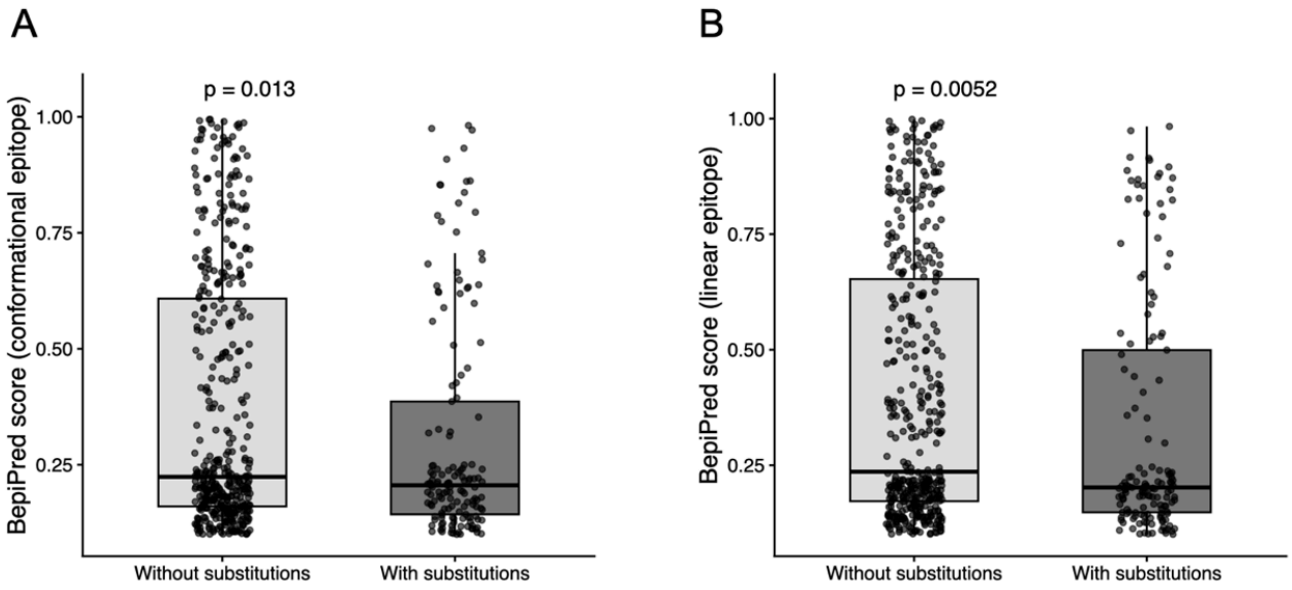


Figure 6

BepiPred-3.0 score distributions for residues with and without substitutions. Boxplots of conformational (A) and linear (B) BepiPred scores (0–1) for residues without and with substitutions.

Supplementary Files

This is a list of supplementary files associated with this preprint. Click to download.

- supplementaryfile.docx